Micellar Structure of Silicone Surfactants in Water from Surface Activity, SANS and Viscosity Studies

ARTICLE *in* THE JOURNAL OF PHYSICAL CHEMISTRY B · FEBRUARY 2002

Impact Factor: 3.3 · DOI: 10.1021/jp0129434

4 AUTHORS:

Saurabh Sureshchandra Soni
Sardar Patel University
37 PUBLICATIONS **548** CITATIONS
SEE PROFILE

Nandhibatla V Sastry
Sardar Patel University
72 PUBLICATIONS **1,462** CITATIONS
SEE PROFILE

Vinod K Aswal
Bhabha Atomic Research Centre
392 PUBLICATIONS **4,906** CITATIONS
SEE PROFILE

Prem Goyal
Pillai Institute of Information Technology, En…
41 PUBLICATIONS **1,044** CITATIONS
SEE PROFILE

Micellar Structure of Silicone Surfactants in Water from Surface Activity, SANS and Viscosity Studies

Saurabh S. Soni,[†] Nandhibatla V. Sastry,*[,†] Vinod K. Aswal,[‡] and Prem S. Goyal[§]

Department of Chemistry, Sardar Patel University, Vallabh Vidyanagar 388 120, Gujarat, India, Solid State Physics Division, Bhabha Atomic Research Center, Mumbai 400 085, India, and Inter University Consortium (IUC) for DAE Facilities, Mumbai Center, Mumbai 400 085, India

Received: July 31, 2001; In Final Form: November 16, 2001

The aqueous solutions of two nonionic silicone surfactants based on polyether modified poly(dimethylsiloxane)s have been analyzed by cloud point, surface tension, small angle neutron scattering (SANS), and viscosity measurements. These surfactants have a comb-like structure with a linear poly(dimethylsiloxane) backbone chain and a grid containing block oligomers of ethylene oxide and/or propylene oxide as branches. The critical micelle concentrations (CMCs) were obtained from break points in surface tension vs log concentration plots and, as expected, decreased systematically with the increase in the hydrophobicity. Small angle neutron scattering (SANS) measurements have been made in aqueous solutions of silicone surfactants at different concentrations (1, 2, and 5 % w/v) and temperatures (30, 45, and 60 °C) to elucidate the structural information on micelles. The analysis of the SANS curves revealed the presence of oblate ellipsoidal micelles in three selected concentrations and temperatures. The size of micelles has strikingly showed a nonvariance in the concentration range of 1−5 % w/v, whereas an increase of 30−60% in the seminor major axis **b** values was noted when the temperature was raised from 30 to 60 °C. Under the same temperature interval, an increase in the aggregation number and a decrease in the number density of micelles were noted. Viscosity measurements also support the presence of aggregates of nonspherical shape. The shape factor for the aggregates calculated from intrinsic viscosities has been found to be in close agreement with the values for the same obtained independently from the SANS measured axial ratios. The micellization of silicone surfactants has been found to be described adequately by closed association process, which was used to obtain the thermodynamic parameters viz. standard free energies (ΔG°_{Mic}), enthalpies (ΔH°_{Mic}), and entropies (ΔS°_{Mic}) of micellization. The micellization process has always been characterized by endothermic enthalpies and thus is driven mainly by entropy factor. The stretching of the core part at elevated temperatures has been attributed to the dehydration phenomenon, as a result of which the water is expelled from the interior of the micelles facilitating the addition of more surfactant molecules into aggregates.

1. Introduction

The surfactants based on oligomeric and/or polymeric molecules have received wide attraction both at academic and industrial scale because of their unique and tailor-made properties over the conventional low molecular weight surface active agents. The oligomeric/polymeric surfactants that exhibit association and self-assembly behavior in water are basically amphiphilic in nature and consist of hydrophobic and hydrophilic moieties within the same molecule. The most common polymer that is used as a hydrophilic part is poly(ethylene oxide) (PEO), which has excellent water solubility up to 100 °C. The hydrophobic moieties have, for example, been either polypropylene oxide (PPO), polybutylene oxide (PBO), poly(dimethylsiloxane) (PDMS), polystyrene (PS), or polyisobutylene (PIB). Of all the di- and tri-block copolymers of PEO−PPO, PEO−PPO−PEO types have been a subject of intensive investigations especially for their self-assembly properties, phase behavior, gelation, etc. The summary of these studies has appeared in the form of excellent and authoritative reviews,[1−4] which cite most of the papers till the recent period. The useful information thus obtained led to the exploration of these pluronic copolymers in widespread industrial applications such as detergency, emulsification, foaming, lubrication, cosmetics, agents for controled release of pharmaceutical formulations, etc.[5]

PEO- and PPO-based block copolymers, which are also known as pluronic surfactants, associate in aqueous media into micellar aggregates, and the micellization can either be induced at a given temperature by increasing the concentration beyond a critical value or at a given concentration beyond a critical micelle temperature. A variety of physical methods[2,6] based on (i) measurements of thermodynamic and other macroscopic properties (heat capacity, viscosity, speeds of ultrasonic sound, surface tension, densities, etc.), (ii) spectroscopic techniques (infrared, Raman, nuclear magnetic resonance, etc.), (iii) scattering techniques such as static and dynamic light scattering, small-angle X-ray scattering, and small angle neutron scattering (SANS), and (iv) other methods such as transient electric birefringence, fluorescence quenching, and dye solubilization can be used for detecting the presence of micelles. Of all these,

* To whom correspondence should be addressed. E-mail: nvsastry_ad1@sancharnet.in.
[†] Sardar Patel University.
[‡] Bhabha Atomic Research Center.
[§] Inter University Consortium.

10.1021/jp0129434 CCC: $22.00
Published on Web 02/14/2002

the third group of methods provide unambiguous information on the size and shape of aggregates formed under varying conditions of temperature, pressure, and solvent quality.[7]

Silicone surfactants or silicone glycols are polyether modified poly(dimethylsiloxane)s.[8,9] The siloxane moiety is soluble neither in water nor in organic oils and thus contributes hydrophobic as well as oleophobic properties to the molecule. The high flexibility of the polysiloxane chain enables it to acquire conformation that results in close and efficient packing at the interface between water/air, oil/air, or water/oil. Moreover silicone glycols could decrease the surface tension of both water as well as organic oils and, hence, they can be used for surfactant action in organic media, in which conventional low molecular weight surfactants as well as PEO−PPO or PEO−PPO−PEO polymeric surfactants are less effective or even some times fail. One another fascinating aspect of silicone surfactants is that the modification of siloxanes can be achieved in a variety of ways to get a wide range of molecular architectures such as comb like siloxanes, α- and ω-functionalized siloxanes, branched siloxanes, or even structures (similar to conventional surfactants), namely, trimethyl- or heptamethyltrisiloxanes. The silicone surfactants have been widely employed as stabilizers for polyurethane foams on one hand and antifoamants in fuels (e.g., diesel) and heavy oils on the other. They also constitute important additives in water as well as nonwater borne coatings. Silicone polyethers with a high content of propylene oxide in the polyether part are used as antifoaming agents in various industrial formulations such as polymer-based dispersions, detergents, paints, and inks. They have also been proven to be efficient wetting agents in spreading aqueous formulations onto hydrophobic substrates.

The wide range of applications of silicone surfactants have been mainly attributed to their high surface activity, low toxicity, and unique association behavior. Despite wide and extensive industrial usage, very little information is available in the literature on the fundamental surfactant properties of silicone glycols in aqueous solutions. To our knowledge, only one report on the aggregation behavior of silicone surfactants in aqueous solutions at 25 °C has been published by Gradzielski et al.[10] The authors have observed that tri- and polysiloxane surfactants form micelles, and their size and shape hardly change in the concentration range of 1−20 wt %. The qualitative analysis of SANS measurements further revealed that micelles were of spherical shape. It is well-known that the size and shape of micelles is very much dependent upon the temperature. As far as we are aware, the effect of temperature on the micelles of silicone surfactants in aqueous media has not been studied so far.

To provide information on the structural characteristics of aggregates formed by silicone surfactants in water and their variation with surfactant concentration and temperature of solution, we report in this paper systematic studies on aqueous solutions of two polyether modified poly(dimethylsiloxane) surfactants by using surface tension, SANS, and viscosity measurements.

2. Experimental Section

2.1. Materials and Sample Preparation. The silicone surfactants were obtained as gift samples from Th. Goldschmidt AG, Germany. They are polyether modified poly(dimethylsiloxane)s. Both samples have a comb like structure as shown in Chart 1.

Values of numbers *m* and *n*, which represent the polyether modified hydrophobic siloxane and hydrophobic poly(dimethylsiloxane) units, and values of *x* and *y* that denote number of ethylene oxide and propylene oxide units in the polyether grid[11] are summarized in Table 1. It can be seen that the hydrophilicity of these surfactants is due to *x* units of ethylene oxide (EO) in a given sample. These products are of industrial origin with an average formula. The values of *m*, *n*, *x*, and *y* are average numbers, and the branch groups A are statistically distributed over the silicone chain. The surfactants were used as received without further purification. Pure poly(dimethylsiloxane)s with 5, 10, and 50 $(CH_3)_2SiO$ units and poly(ethylene oxide) samples having 1000 and 3400 g mol^{-1} of molecular weights were obtained from Aldrich Chemical Co. and were used as such with out any purification.

CHART 1: Structure of Silicone Surfactants

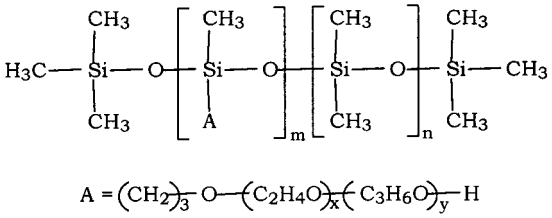

TABLE 1: Molecular Parameters, Number of Polyether Modified Siloxane, *m*, Poly(dimethylsiloxane), *n*, Ethylene Oxide (EO), *x*, and Propylene Oxide (PO), *y*, Units and Molecular Weight of Silicone Surfactants

silicone surfactant	*m*	*n*	*x*	*y*	% EO	mol. wt, g mol^{-1}
SS-1	5	13	12	0	100	4360
SS-2	5	20	10	4	75	5600

Water, freshly triple distilled from an all Pyrex glass still (or D_2O for SANS experiments), was used in preparing stock solutions (of 10 wt %) in stoppered glass vials. The stock solution was allowed to be stirred on a magnetic stirrer until homogeneous and thorough mixing is achieved. A stirring period of 60−90 min was found to be sufficient. After the stock solution was allowed to stand for a day, dilutions were made to get the desired concentrations. The solutions were always stored in stoppered glass vials. We did not detect any hydrolysis in the surfactant solutions at least for 4 weeks.

2.2. Methods. The surface tension of silicone surfactant solutions was measured by drop weight method using a modified stalagmometer.[12] The stalagmometer assembly consists of Pyrex glass bulb of spherical shape with a capillary tube attached at filling and dropping ends. The capillary tube at the dropping end is blown into a 2-fold U shape, and the tip of the end is grounded in the form of a fine cone. By this way, not only is the formation of drops of uniform shape and size ensured but also drops are allowed to break under their own weight. A thoroughly stoppered weighing bottle is attached to the dropping end through a rubber septum. The weighing bottle attached to a dropping capillary tube was placed suspended in another closed long glass tube. The stalagmometer assembly along with the predried and preweighed weighing bottle was lowered into a thermostatic water bath maintained at the desired temperature accurate to ±0.01 °C. A 30 min time of equilibration was always allowed. Then a known number of drops (>20) of given solution and reference triple distilled water were allowed to fall into the weighing bottle in separate runs. The weight of solutions as well as triple distilled water drawn from separate runs was instantly recorded on single pan balance. The weight measurements were accurate to ±0.000 01 g. The surface tension of the individual solution was then calculated from known values of surface tension of water, densities, and weights of solution

and water. The stalagmometer was tested for pure and reference organic liquids (carbon tetrachloride, *n*-hexane, etc.) and also sodium dodecyl sulfate aqueous solutions. The surface tensions calculated by this method are found to be within ±0.2% limits of literature reported values of reference liquids.[13]

The SANS experiments were carried out on micellar solutions prepared by dissolving known amounts of surfactants in D_2O. D_2O (with at least 99.5 atom % purity) was obtained from the heavy water division of BARC, Mumbai, India. The use of D_2O instead of H_2O for preparing solutions provides a very good contrast between solute aggregates and solvent in a SANS experiment. SANS measurements were carried out using SANS spectrometer at the DHRUVA Reactor, (Trombay, India).[14] The solutions were held in 0.5 cm path length UV-grade quartz sample holders with tight-fitting Teflon stoppers, sealed with Parafilm. The sample to detector distance was 1.8 m for all runs. The spectrometer makes use of a BeO filtered beam and has a resolution ($\Delta\mathbf{Q}/\mathbf{Q}$) of about 30% at $\mathbf{Q} = 0.05$ Å^{-1}. The angular distribution of the scattered neutron is recorded using an indigenously built one-dimensional position-sensitive detector. The accessible wave transfer $\mathbf{Q}$ ($= 4\pi \sin 0.5\theta/\lambda$, where λ is the wavelength of the incident neutrons and θ is the scattering angle) range of this instrument is between 0.02 and 0.3 Å^{-1}. The mean neutron wavelength was $\lambda = 5.2$ Å.

SANS measurements with a given surfactant solution were made at three different temperatures. Similarly, at a given temperature, the concentration of the surfactant was varied. The measured scattering intensities of neutrons were corrected for the background, empty cell scattering, and sample transmission. The intensities then were normalized to absolute cross-section units. Thus, plots of $d\Sigma/d\Omega$ vs $\mathbf{Q}$ were obtained. The uncertainty in the measured scattering intensities is estimated to be 10%. The experimental points are fitted using a nonlinear least-squares method.

The flow times of surfactant solutions and water were obtained by using Ubbelohde suspended level viscometers. Two viscometers were used to record flow times in the range of 130−360 s, thus avoiding any kinetic corrections. Three consecutive flow times agreeing within ±0.02 s were taken and the mean flow time was considered. Shear corrections were not taken into consideration because obtained intrinsic viscosities were always less than 3 dL g^{-1}. The flow volume was greater than 5 mL, making drainage corrections unimportant. Viscometers were suspended in thermostatic water baths maintained at constant temperature accurate to ±0.01 °C. The densities of aqueous surfactant solutions were measured by using high precision Anton Paar Densitymeter DMA 5000. The measured densities are accurate to ±0.000 001 g cm^{-3}, and the temperature during the measurements has a precision of ±0.001 °C.

3. Results and Discussion

The phase diagrams for the dilute aqueous solutions of silicone surfactants were constructed by visual examination of changes in the physical appearance of solution with temperature. Such diagrams for both the surfactants are shown in parts a and b of Figure 1. The nature of curves presented in the figure showed that both surfactants follow a similar trend. Solutions in the concentration range (0.1−10 wt %) studied remain isotropic and clear initially, then turn turbid, and become cloudy, and at high temperatures, clouds became more dense. The temperature at which dense clouds were noted is considered as the cloud point (C_p). It is interesting to note that the dense clouds once formed remain stable with out any phase separation up to temperatures close to 95 °C.

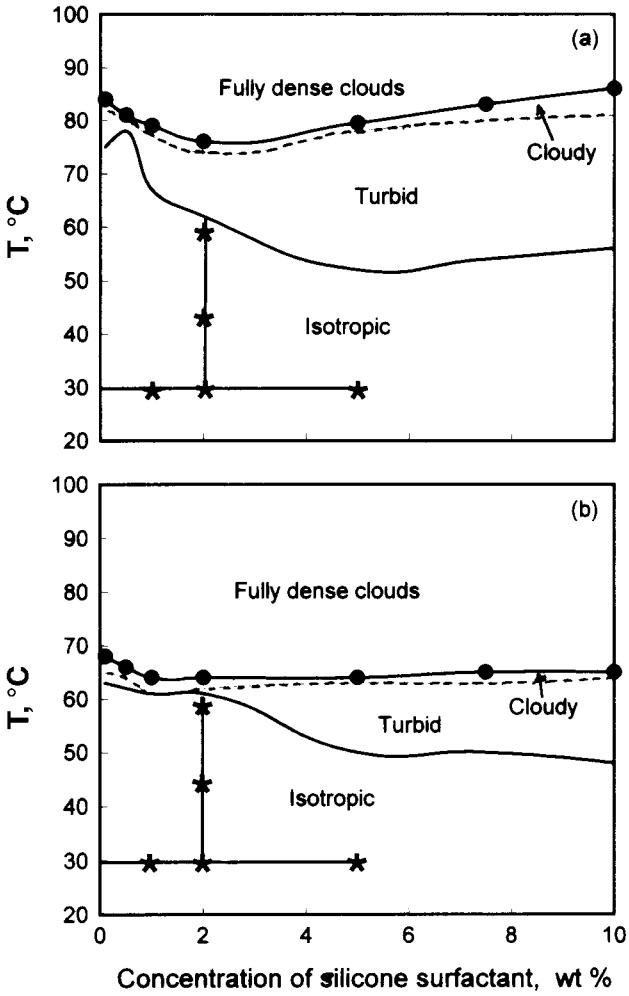

Figure 1. Phase diagram of the silicone surfactants, (a) SS-1 and (b) SS-2, in dilute aqueous solutions. Final cloud points for SS-1 (●) and SS-2 (●) surfactant solutions. Crosses on the horizontal line indicate the concentrations and on the vertical line indicate the temperatures corresponding to SANS measurements.

Pure poly(dimethylsiloxane)s with an average 5, 10, and 50 $(CH_3)_2SiO$ units are liquids and show poor miscibility with water in the concentration range of 0.1−5 wt % and in a temperature interval of 7−80 °C. The liquids when mixed with water form a sticky separate layer on the top of the water surface which splits into fine and suspending droplets upon agitation. The silicone surfactants, which are polyether modified poly(dimethylsiloxane)s, however, showed good solubility in water, indicating enhanced dispersibility of poly(dimethylsiloxane) units in water. The solubility as well as good dispersibility of silicone surfactants in water is thus dependent essentially on the ethylene oxide content in the polyether grid. The increase in temperature is expected to produce mainly two effects on silicone surfactant solutions: (i) the dehydration of ethylene oxide as well as propylene oxide units in the polyether grid and (ii) a decrease in dispersibility or miscibility of dimethyl siloxane units. Aqueous solutions (of 0.5−10 wt % concentrations) of poly(ethylene oxide) samples with 1000 and 3400 g mol^{-1} molecular weights have been found to be clear and transparent with no turbidity or visible phase separation from 5 to 90 °C temperature interval.

The silicone surfactant samples SS-1 and SS-2, on average, have 60 and 50 $-(CH_2CH_2O)-$ units. From the above recorded observations on the solutions of pure poly(dimethylsiloxane) and poly(ethylene oxide) samples, it can be stated that the

ethylene oxide part of the silicone surfactants is mainly responsible for their over all solubility in water up to the temperature and concentration range, marked by curve 1. The appearance of turbidity in solutions between the temperature limit of curves 1 and 2 and of clouds beyond curve 2 cannot be directly accounted by the possible dehydration effect on thePEO part alone because the solutions of PEO homopolymers did not show any phase separation in the temperature interval of 15−95 °C. Then the very fact that solutions of SS-1 and SS-2 become turbid with rise in temperature means that the miscibility of the silicone part of the surfactant weakens at elevated temperatures. The observed cloudiness with further rise in temperature beyond the turbidity appearance needs to be accounted for. If silicone surfactants form micelles and a full characterization of these aggregates in terms of their size and shape can be made, then the information on the concentration and temperature dependence of the micellar parameters is expected to throw some light on the nature of the process that leads to the clouding behavior of these surfactants.

In present investigation, an attempt has been made through surface tension, SANS, and viscosity measurements to characterize the solutions of silicone surfactants in the region of the phase diagram corresponding to transparent and isotropic states. The range of concentrations studied at a fixed temperature of 30 °C and temperature variations at a fixed concentration for SANS and viscosity measurements is shown as horizontal and vertical lines in Figure 1.

Of all of the methods that can be used for estimating CMC, the surface tension method is versatile because not only can the CMC be extracted from plots of surface tension versus log concentration but also one can get information on the nature of adsorbed layers at the air/water interface.[15] The typical plots of surface tension versus log concentration for aqueous solutions of silicone surfactants SS-1 and SS-2 at 15, 25, and 45 °C are shown in parts a and b of Figure 2. Also included for comparison purposes are surface tension values for the pure PEO homopolymer sample of molecular weight 3400 g mol^{-1} at the same temperatures. The plots shown in the figure are typical in nature. The variation of surface tension values over several decades of concentration for both silicone surfactants followed the same trend at three temperatures. The surface tension values decrease linearly with the logarithm of the surfactant concentration and show a characteristic break and remain constant thereafter. Further examination of the plots reveals a systematic increase in surface tension values with an increase in temperature and at the same time a shift in break points to lower values. In contrast, the surface tension values monotonically decrease with an increase in concentration from 0.001 to 10 wt % for pure PEO homopolymer samples. There are not many reports available in the literature on the surface tension versus concentration profiles for aqueous solutions of silicone surfactants with which we can make a direct comparison. Gradzielski et al.[10] have constructed surface tension versus concentration profiles at 25 °C, for a series of silicone surfactants with different molecular architectures, i.e., short siloxane backbone (cationic, anionic, and zwitterionic) and long siloxane backbone polyether modified nonionic siloxanes, etc. The authors have noted characteristic break points in the plots for all of the silicone surfactants. These break points have been attributed to CMC values for short chain trisiloxane surfactants. When an energy value of 12.1 kT for the transfer of an hydrophobic group from water to micelle interior was taken, a CMC value (of $<10^{-26}$ mol dm^{-3}) was predicted for one of the long backbone containing poly(dimethylsiloxane)−polyether (CL 681).

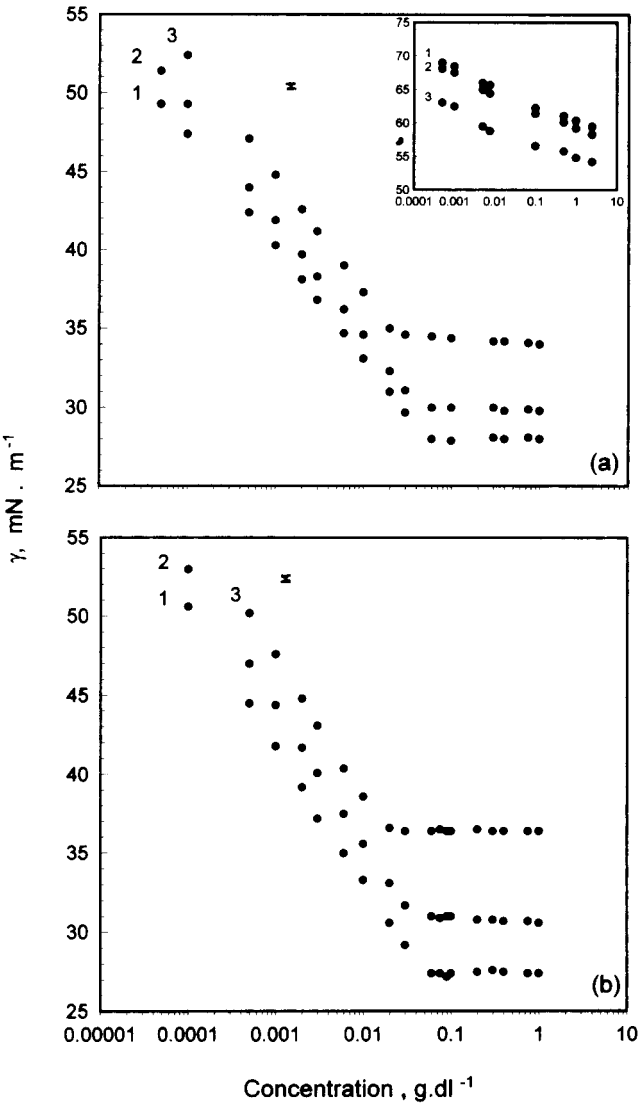

Figure 2. Plots of surface tension versus logarithm concentration for silicone surfactants aqueous solutions of (a) SS-1 and (b) SS-2 at different temperatures: 15 (1), 25 (2), and 45 °C (3). Curves for pure PEO (mol. wt 3400 g mol^{-1}) aqueous solutions are shown in the figure inside. The markings in the figure are estimated errors in γ.

CL-681 has similar architecture and molecular characteristics with one of the surfactants studied, i.e., SS-1 in the present investigation. Interestingly, authors had in fact noted a sharp break in plots of surface tension versus log CL-681 concentration at a value less than 1.1×10^{-6} mol dm^{-3} which is almost 10^{-21} times more than expected. They did not account any reason for this observed discrepancy. Kanellopoulos and Owen[16] have also measured surface tensions of aqueous solutions of ABA type block copolymers where A is poly(dimethylsiloxane) and B is a polyether, at 25 °C. The polyether block itself was a random poly(ethylene oxide)−polypropylene oxide copolymer having on an average 44 oxyalkylene units per segment. The surface tension versus concentration plots for a series of copolymers with increasing siloxane content were typical "L" shape with well defined and sharp break points. A systematic decrease of CMC with an increase in the number of dimethylsiloxane units was noted. A very low CMC contrary to an expected high value for a sample having $n = 12.5$ units was accounted for by considering that dimethylsiloxane chains with a higher degree of polymerization, i.e., $n > 22$, form a closely packed doubly coiled monolayer and when $n < 20$ the polysiloxane chain length

TABLE 2: Values of CMC, CMC/C_{20}, Surface Excess Concentration, Γ_m, Area Per Copolymer Molecules, a_1^s, Surface Pressure, π, Free Energy, ΔG^0_{Mic}, Enthalpy, ΔH^0_{Mic}, and Entropy, ΔS^0_{Mic}, of Micellization at Different Temperatures

surfactants	temp, °C	CMC, g dl^{-1}	CMC/C_{20}	$\Gamma_m \times 10^{10}$, mol cm^{-2}	a_1^s, Å^2	π_{CMC}, mN m^{-1}	ΔG^0_{Mic}, kJ mol^{-1}	ΔH^0_{Mic}, kJ mol^{-1}	ΔS^0_{Mic}, kJ K^{-1} mol^{-1}
SS-1	15	0.054 ± 0.003	2279	1.3 ± 0.1	129 ± 5	45.4 ± 0.1	−31.1	34.9	0.2
	25	0.040 ± 0.004	712	1.3 ± 0.1	129 ± 3	41.2 ± 0.1	−33.0	37.4	0.2
	45	0.025 ± 0.002	59	1.2 ± 0.1	133 ± 4	34.0 ± 0.1	−36.4	42.6	0.3
SS-2	15	0.047 ± 0.004	836	1.6 ± 0.1	106 ± 3	46.0 ± 0.1	−32.1	50.0	0.3
	25	0.034 ± 0.003	250	1.5 ± 0.1	110 ± 2	41.2 ± 0.1	−34.0	53.5	0.3
	45	0.016 ± 0.002	22	1.5 ± 0.1	114 ± 3	32.0 ± 0.1	−38.2	60.9	0.3

may be too less for the formation of above-mentioned type monolayer and, hence, could be highly surface active (and thus have low CMC values). SS-1 and SS-2 surfactants not only differ in composition of dimethylsiloxane and polyether units but also in the molecular architecture. SS-1 and SS-2 are branched polymers in contrast to the triblock copolymeric nature of polyether−poly(dimethylsiloxane)−polyether used by Kanellopoulos and Owen. Hence, under these conditions, a direct comparison of our data is not worthwhile. However, the "L" type nature of surface tension versus logarithm concentration plots observed for our samples is in excellent qualitative agreement with the same profiles reported by Kanellopoulos and Owen.

The CMC data along with other extracted surface active parameters from the profiles shown in Figure 2 are listed in Table 2. The ratio between the molecular weights of hydrophobic to hydrophilic parts for SS-1 and SS-2 surfactants are 0.65 and 1.55, respectively. A perusal of data presented in Table 2 shows that CMC values decrease systematically with the increase in hydrophobicity of silicone surfactants. Kanellopoulous and Owen[16] have also reported a similar trend in CMC values with the increase in the hydrophobicity for a series of triblock polyether−poly(dimethylsiloxane)s having narrow molecular weight distribution. A rise in temperature from 15 to 45 °C, is found to decrease CMC values almost by more than two times. These observations clearly indicate that the length of the hydrophobic part in the silicone surfactants plays a crucial role in the micelle formation. The larger the hydrophobicity of surfactants, the smaller the concentration at which the micelles are formed. Similar conclusions have been drawn for PEO−PPO−PEO pluronic surfactans.[17−19]

To elicit the information on the preferred orientation of silicone surfactant molecule at air/water interface, the surface excess concentration, Γ_m, and the area per molecule, a_1^S, at the air/water interface are also calculated by using Gibbs equation[1]

$$\Gamma_m = -\frac{1}{2.303RT}\left(\frac{\partial\gamma}{\partial \log C}\right)_T \qquad (1)$$

and

$$a_1^s = \frac{10^{16}}{N\Gamma_m} \qquad (2)$$

where $R = 8.31$ J mol^{-1} K^{-1}, T = absolute temperature in °K, γ = surface tension values in mN m^{-1}, C = concentration in mol dm^{-3}, and N = Avogadro's number. Γ_m is expressed in mol cm^{-2}. In these calculations, the estimated area per molecule will be an averaged value because the values of *m*, *n*, *x*, and *y* in SS-1 and SS-2 samples (please refer Chart 1) are averaged and also the branched part of A is randomly distributed along the chain. The slope values needed in the calculation of Γ_m have been obtained from the linear portion of the plots.

The analysis and interpretation of surface area per molecule and its dependence on hydrophobicity of branched silicone surfactants and temperature are not straightforward because of the complexity of their molecular architecture. The a_1^s for SS-1 surfactant is almost invariant with the temperature, whereas for SS-2 surfactant molecules, it shows an increase by 3−6% with rise in temperature from 15 to 45 °C. It is difficult to ascertain whether which single or all of the moieties, i.e., CH_3SiAO, (C_2H_4O) attached as a part of A to CH_3SiO and $(H_3C)_3SiO$ adjacent to the hydrophilic branches contribute to the measured surface area values. The surface areas for simple nonionic alkyl polyether surfactants having a hexadecyl hydrophobic chain alongside 63 ethylene oxide units (which act as hydrophilic moieties) have been reported to be 130 Å^2 at 10 °C and gradually increased to 132, 137, 141, and 143 Å^2 at 18, 25, 33, and 40 °C temperatures, respectively.[20] The SS-1 surfactant has total of 25 hydrophobic [methyl and methylene parts of $(CH_3)_3SiO$, $(CH_3)_2SiO$, $(CH_2)_3O$, and $(CH_3)_3Si$] and 60 hydrophilic (CH_2-CH_2O) units, whereas the SS-2 surfactant consists of 52 hydrophobic [methyl and methylene parts of $(CH_3)_3SiO$, $(CH_3)_2$-SiO, $(CH_2)_3O$, $(CH_3)_3Si$, and (C_3H_6O)] and 50 hydrophilic (CH_2-CH_2O) groups. Upon comparison of our observed values of surface areas occupied by SS-1 and SS-2 surfactant molecules with that of nonionic $C_{16}O(EO)_{63}$, it is found that SS-1 surfactant molecules have almost same occupied area value, whereas SS-2 surfactant molecules seem to adsorb at the air/water interface with lower (about 23−19 Å^2) occupied areas. Barry and El Eini[20] envisaged that $C_{16}O(EO)_n$ (n = 17−63) surfactants adsorb at the air/water interface with the hydrophilic (EO) units probably oriented parallel to the surface, with one end anchored by the hydrophobic alkyl chain projecting outward and the other end tending to move away from the surface into the bulk. The similarity in surface areas between the SS-1 silicone surfactant which has a close resemblance (in number (60) of hydrophilic units) to that of $C_{16}O(EO)_{63}$ would suggest that the preferred orientation of SS-1 molecules at the air/water interface would be the same to that of alkyl polyethers as described above.

The major question that still remains unanswered is what could be the nature of the orientation of Si−O linkage at the air/water interface? Gradzielski et al.[10] have concluded that the Si−O groups are neither hydrophobic nor hydrophilic and the total hydrophobic effect of the silicone surfactants is due to $-CH_3$ and $-CH_2$ groups attached to siloxane chain. It has also been observed[15] that for each addition of a hydrophobic $-CH_2-$ group to the alkyl chain, in alkyloctaethyleneglycol ethers, the surface area per adsorbed molecule decreases by 6−7 Å, when the surfactant molecule has a linear structure. One cannot thus directly extend this rationale to SS-1 and SS-2 surfactants because they have a complex branched molecular architecture. Moreover, for linear triblock PEO−PPO−PEO copolymers, the surface areas have been found to decrease drastically with increase in temperature.[18,19] We did not notice this type of temperature dependence either for our samples. However, the

L shape of the plots (Figure 2) with a well defined and single sharp break point are similar to those of linear alkyloctaethyleneglycol ethers. Pluronic surfactants have been reported to exhibit two break points in γ vs log C plots.[17,19,22] Thus. we, at present, cannot make any generalization about the nature of adsorbed layer at the air/water interface formed by silicone surfactants. More studies covering a wide range of hydrophobicites among similar architectured silicone surfactants are needed for a clear understanding. However, the observed L shape plots and higher a_l^s values for SS-1 and SS-2 surfactants (in contrast to their alkypolyether counterparts) hint that Si−O groups of hydrophobic parts probably may tend to orient preferentially toward the water surface because of hydration effects and that the adsorbed layers have a compressed nature.[21]

The characteristic CMC/C_{20} ratio values for SS-1 and SS-2 surfactants were estimated to be 0.040 and 0.034 at 25 °C and are far less than that of similar ratios (of the order of 10^4 magnitude) calculated for pluronic copolymers of F-38 ($(PEO)_{42}$-$(PPO)_{16}(PEO)_{42}$)[18] and P-85 ($(PEO)_{26}(PPO)_{39}(PEO)_{26}$).[19] It has been generally noted that the lower the CMC/C_{20} ratio, the less the CMC will be, and the converse is also true. Hence, it can be inferred that SS-1 and SS-2 surfactant molecules saturate the surface even with lower concentration, and a further increase in the later will result in the formation of micellar aggregates. Another interesting feature of CMC/C_{20} values is that they get drastically decreased to 59 and 22 from 2279 and 836 for SS-1 and SS-2 surfactants, respectively, when the temperature is raised from 15 to 45 °C. As noted earlier, the effects of temperature on a_l^s values is very marginal under the same conditions. Strong temperature dependence of CMC/C_{20} has also been reported for alkylpolythers[15] and pluronic PEO−PPO−PEO surfactants.[19] The rise in temperature promotes loss of hydration water, weakens the cohesion among water molecules, and, hence, facilitates the formation of compressed adsorbed layers with lower surface areas.[19,23] Though dehydration effects are expected in silicone surfactant aqueous solutions, the observed quasiconstant or slight increasing trend in a_1^s values can only be attributed probably to a greater flexibility of Si−O−Si linkage with rise in temperature (it may be noted that the Si−O bond length of 0.165 nm is more as compared to 0.140 nm for a C−C bond, and also, the Si−O−Si bond angle of 130° is higher than the C−O−C bond angle of 110° in dimethyl ether). The enhanced mobility of siloxane groups at elevated temperatures decompresses the adsorbed layer and decreases the surface activity which results in higher surface tension values (as noted in Figure 2).

The last three columns of Table 2 list various thermodynamic parameters viz. free energy, $\Delta G°_{Mic}$, enthalpy, $\Delta H°_{Mic}$, and entropy, $\Delta S°_{Mic}$, of micellization for both the silicone surfactants calculated using following relations derived from pseudo phase separation and mass action models

$$\Delta G°_{Mic} = RT \ln\left(\frac{CMC}{\omega}\right) \tag{3}$$

where ω is the molarity of water

$$\Delta H°_{Mic} = -2RT^2\left(\frac{\partial \ln CMC}{\partial T}\right) \tag{4}$$

and

$$\Delta S°_{Mic} = \left(\frac{\Delta H°_{Mic} - \Delta G°_{Mic}}{T}\right) \tag{5}$$

The $\Delta G°_{Mic}$ values are always negative and become more negative with a rise in temperature from 15 to 45 °C. This indicates that the tendency of micellization increases with enhanced hydrophobicity of $(CH_3)_2SiO$, C_4H_6O, and also of C_2H_4O groups as a consequence of dehydration effects. Similar is the trend in $\Delta G°_{Mic}$, in which it becomes slightly more negative when the length of the hydrophobic part is increased from the SS-1 to the SS-2 surfactant. The $\Delta H°_{Mic}$ values are positive and increase with the rise in temperature for a given silicone surfactant micelles and also with the lengthening of the hydrophobic part of the chain from SS-1 to SS-2. Because the enthalpy values are highly positive and, hence, unfavorable for micellization, the negative $\Delta G°_{Mic}$ must have a predominant contribution from the observed positive entropy of micellization, $\Delta S°_{Mic}$. Thus, it can be stated that micellization of silicone surfactants is entropy-driven as in the case with the self-assembly behavior of classical low molecular weight surfactants[15] and also pluronic-based polymeric surfactants.[4]

3.1. SANS Measurements. SANS method is a powerful technique for getting structural information especially on micellar aggregates.[24] To obtain information on the shape, size, and variation with the concentration and temperature, SANS measurements have been made in aqueous solutions of silicone surfactants, SS-1 and SS-2, over a concentration range of 1−5 wt % and temperature limit of 30−60 °C. While carrying out SANS measurements, care has been taken to ensure that the solutions are transparent in appearance. By this way, we hope that the complex macroscopic effects that may arise because of phase separation (or clouding) would be eliminated.

3.1.1. Theory of SANS and Expressions for SANS Scattering Cross-Section. SANS experiment measures the coherent differential scattering cross-section $d\Sigma/d\Omega$ for the sample. The expression for $d\Sigma/d\Omega$ for a unit volume of solution of monodisperse spherical micelles is given by[24,25]

$$\frac{d\Sigma}{d\Omega} = \mathbf{n}_m \mathbf{V}^2_m(\rho_m - \rho_s)^2\{\langle \mathbf{F}^2(\mathbf{Q})\rangle + \langle \mathbf{F}(\mathbf{Q})\rangle^2 [\mathbf{S}(\mathbf{Q}) - 1]\} + \mathbf{B} \tag{6}$$

where $\mathbf{n}_m$ denotes the number density of the micelles and ρ_m and ρ_s are the scattering length densities of the micelles and the solvent, respectively. $\mathbf{F}(\mathbf{Q})$ is the single particle (intraparticle) form factor, $\mathbf{S}(\mathbf{Q})$ is the interparticle structure factor, and $\mathbf{B}$ is a constant term that represents the incoherent scattering background, which is mainly due to the hydrogen in the sample.

The particle form factor $\mathbf{F}(\mathbf{Q})$ depends on the shape and size of the micelles. Expressions for $\mathbf{F}(\mathbf{Q})$ corresponding to different geometrical shapes are known.[26,27] In particular, $\mathbf{F}(\mathbf{Q})$ for an ellipsoidal micelle is given as

$$\langle \mathbf{F}^2(\mathbf{Q})\rangle = \int_0^1 [\mathbf{F}(\mathbf{Q}, \mu)]^2 \, d\mu \tag{7}$$

$$\langle \mathbf{F}(\mathbf{Q})\rangle^2 = [\int_0^1 \mathbf{F}(\mathbf{Q}, \mu) \, d\mu]^2 \tag{8}$$

$$\mathbf{F}(\mathbf{Q}, \mu) = \frac{3 (\sin x - x \cos x)}{x^3} \tag{9}$$

$$x = \mathbf{Q}[\mathbf{a}^2\mu^2 + \mathbf{b}^2(1 - \mu^2)]^{1/2} \tag{10}$$

where $\mathbf{a}$ and $\mathbf{b}$ are, respectively, the semiminor and semimajor axis of the ellipsoidal micelle and μ is the cosine of the angle between the major axis and the wave reactor transfer $\mathbf{Q}$.

We would like to mention that, although $\mathbf{F}(\mathbf{Q})$ at small $\mathbf{Q}$ is sensitive to the dimension of the major axis, its behavior at large $\mathbf{Q}$ is decided by the dimension of the minor axis of the micelles.

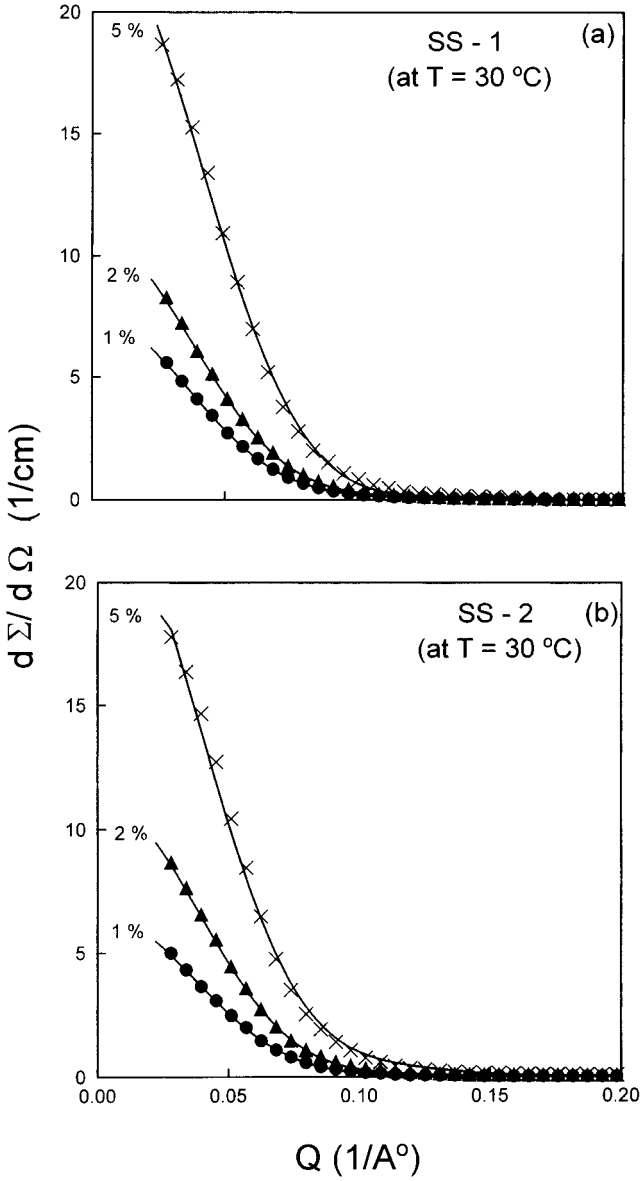

Figure 3. SANS distributions from micelles of silicone surfactants, (a) SS-1 and (b) SS-2, at different concentrations at 30 °C. The curves are fitted values using the oblate ellipsoidal cross section formula of eq 11.

S(**Q**), the interparticle structure factor, is decided by the spatial arrangement of micelles in solution. Usually, **S**(**Q**) shows a peak at $\mathbf{Q}_m = 2\pi/D$, where D is the average distance between micelles. Thus, the peak in the **S**(**Q**) usually shifts to higher **Q** values with an increase in surfactant concentration. It may be mentioned that the spatial arrangement of micelles and the **S**(**Q**) depends on the intermicellar interactions. In principle, interaction potential, $V(r)$ between micelles could change with temperature of the solution. That is, a change in temperature could also result in changes in **S**(**Q**).

3.1.2. Analysis of SANS Data. 3.1.2a. Concentration Dependence. The characteristic neutron scattering curves for SS-1 and SS-2 aqueous solutions at different concentrations of 1, 2, and 5 wt % and at 30 °C are shown in parts a and b of Figure 3. The curves for SS-1 and SS-2 surfactants have common characteristics at all of the three concentrations. The coherent differential scattering cross section ($d\Sigma/d\Omega$) (which is also often referred as intensity) shows relatively strong **Q** dependence. The measured SANS distribution is typical of that obtained from micellar solutions.[28−30] In view of this and the fact that scattering cross-sections of individual polymer molecules are much smaller than those seen above, it is suggested that surfactant molecules are aggregating to form micelles. It is seen that SANS distribution at high **Q** is almost independent of surfactant concentration. This suggests that at least one of the dimensions of the micelle is independent of surfactant concentration.

It may be noted that the micelles of silicone surfactants are expected to be consisting of a hydrophobic core part and a hydrated corona surrounding the former. As it is evident from the chemical structure of silicone surfactants (please see Chart 1), the hydrophobic core must consist backbone units of dimethylsiloxane, dimethylsilane, and also the spacer group $(CH_2)_3O$ plus y units of propylene oxide (PPO). The surfactant SS-1 has zero PPO units, and SS-2 has four PPO units. Keeping the comblike structure in mind, one can visualize that the micellar corona in SS-2 micelles at ambient temperatures has to be drawn inward to accommodate the PPO units into the core part. For the SANS experiments, surfactant solutions are prepared in D_2O, and there is a good contrast between the hydrophobic core and the solvent on one hand and a poor contrast between the hydrated corona part and the solvent media on the other. Consequently, the value of **F**(**Q**) depends only on the size and shape of the hydrophobic core. Thus, the ratio between micellar volume, V_m, and the volume of hydrophobic part of surfactant monomeric molecule, ν, gives the aggregation number, N_{agg}, of the micelles.

The measured SANS distributions (Figure 3) are monotonically decreasing with **Q**, and there is no indication of the correlation peak. This suggests that for the concentrations reported in this paper intermicellar interference effects are negligible. Thus, we have assumed $\mathbf{S}(\mathbf{Q}) = 1$ in further analysis.

The measured distributions were thus fitted to the following expression:

$$\frac{d\Sigma}{d\Omega} = \mathbf{n}_m \mathbf{V}^2_m (\rho_m - \rho_s)^2 \langle \mathbf{F}^2(\mathbf{Q}) \rangle + \mathbf{B} \qquad (11)$$

F(**Q**) was calculated assuming spherical, ellipsoidal (prolate and oblate), cylindrical, and disk shapes for the micelles. ρ_s for the solvent has a value of 6.38×10^{10} cm^{-2}, and the value of ρ_m was calculated assuming that scattering is from the hydrophobic core of the micelle, and no other variation in contrast was invoked while comparing the calculated and the experimental data. Then the correlation between calculated and experimental values of scattering intensities is judged by calculating χ^2 values. The quantity χ^2 is defined by the following expression:

$$\chi^2 = (1/M - K) \sum [I_{cal} - I_{exp}/(E(I_{exp}))]^2 \qquad (12)$$

where M = number of points, K = number of fitting parameters (i.e., two in the present case), I = intensities, and E = error in I measurements.

It was found that our experimental SANS intensities were best matched with the values obtained by using an oblate ellipsoidal model. The following rigorous procedure was adopted in obtaining the final values of **a** and **b**. By considering, **a** and **b** as adjustable parameters, an initial estimate for both of them was obtained. It was further found that for a different initial set of values of **a** and **b** almost the same value of **a** was obtained. Then the value of **a** is frozen or kept constant, and at the same time, the value of **b** is varied as an input parameter. The aggregation number, N_{agg}, of the micelles is then calculated as

$$N_{agg} = V_m/V_h \qquad (13)$$

TABLE 3: Values of Semimajor Axis, b, Semiminor Axis, a, Axial Ratio, b/a, Aggregation Number, N_{agg}, and Number Density, n_m, of the Oblate Ellipsoidal Micelles of Silicone Surfactants at 30 °C

conc., (wt %)	**b**, Å	**a**, Å	b/a	N_{agg}	$\mathbf{n}_m$, cm^{-3}
			SS-1		
1	51	23	2.2	95	1.456×10^{16}
2	50	23	2.2	92	3.007×10^{16}
5	48	23	2.1	85	8.432×10^{16}
			SS-2		
1	49	25	2.0	47	2.289×10^{16}
2	48	25	1.9	45	4.780×10^{16}
5	46	25	1.8	41	13.117×10^{16}

where V_m is the micellar volume which equals $4/3\pi\mathbf{ab}^2$ and V_h is the volume of hydrophobic parts, i.e., $(CH_3)_3SiO$, $(CH_3)_2SiO$, and $(CH_2)_3O$ units and one unit of $(CH_3)_3Si$. From the estimated values of N_{agg}, the number density of micelles, $\mathbf{n}_m$, i.e., the number of surfactant molecules per unit volume, is calculated by the following relation:

$$\mathbf{n}_m/\mathrm{cm}^{-3} = \frac{CN_A \times 10^{-3}}{N_{agg}} \tag{14}$$

where C = concentration in mol dm^{-3} and N_A = Avogadro's number.

All of the parameters that characterize the micellar aggregates of silicone surfactants, as extracted from the above procedure, are listed in Table 3. Interestingly, a perusal of the data shows that the values of **b**, **a**, and, hence, **b**/**a** are nearly constant in the concentration range of 1−5 wt %. The noted small decrease of about 3 Å in 5 wt % solution is within the experimental uncertainty limits of 10% in the measured intensities.

Under the condition $\mathbf{S}(\mathbf{Q}) = 1$, a look at eq 11 used for evaluating the theoretical scattering intensities reveals that the $d\Sigma/d\Omega$ can be considered proportional to $\mathbf{F}(\mathbf{Q})$ when the terms $\mathbf{n}_m$, V_m, and $(\rho_m - \rho_s)$ are constants. As the shape and size of micelles and hence $\mathbf{F}(\mathbf{Q})$ do not change with concentration, the observed enhanced intensities can be accounted by a corresponding change in the number density of the micelles. Indeed the last column of Table 3 shows about a 5- to 6-fold increase in $\mathbf{n}_m$ values when the concentration is varied from 1 to 5 wt %. The theory of micellization based on the closed association model predicts a similar increase in the number density of nonspherical globular (or ellipsoidal) micelles with increase in concentration.[31]

Gradzielski et al.[10] have monitored the aggregation behavior of several types (ionic as well as nonionic and short chain and long chain polyether modified siloxanes) of silicone surfactants at 25 °C using SANS measurements. The authors have also noted a strong **Q** dependence of scattering intensities. A quantitative analysis of $\mathbf{I}(\mathbf{Q})$ versus **Q** curves was made assuming spherical shape for the aggregates. No analytical model was applied by them to compute the $\mathbf{F}(\mathbf{Q})$ factor. Incidentally, the size, shape, and aggregation number of the nonionic long backbone siloxane−polyether silicone surfactants (CL 680, CL 681, and CL 630), extracted from the qualitative analysis, were found to be independent of concentration, and at the same time, the calculated number density of aggregates increased at high concentration. On the basis of these results, the authors have concluded that the aggregates cannot be of perfect spherical form and may have an ellipsoidal shape. One of the surfactants, namely, CL 681, as noted earlier, is similar in molecular characteristics to one of our samples, SS-1. When we analyzed the scattering curves by assuming a spherical shape for the $\mathbf{F}(\mathbf{Q})$, the χ^2 values were found to be as large as 31.35. Hence, the spherical shape for the aggregates is ruled out. We believe that Gradzielski et al.[10] did not model fit their SANS data correctly; otherwise, their conclusions about the size and shape of nonionic silicone surfactant micelles could have been similar to ours.

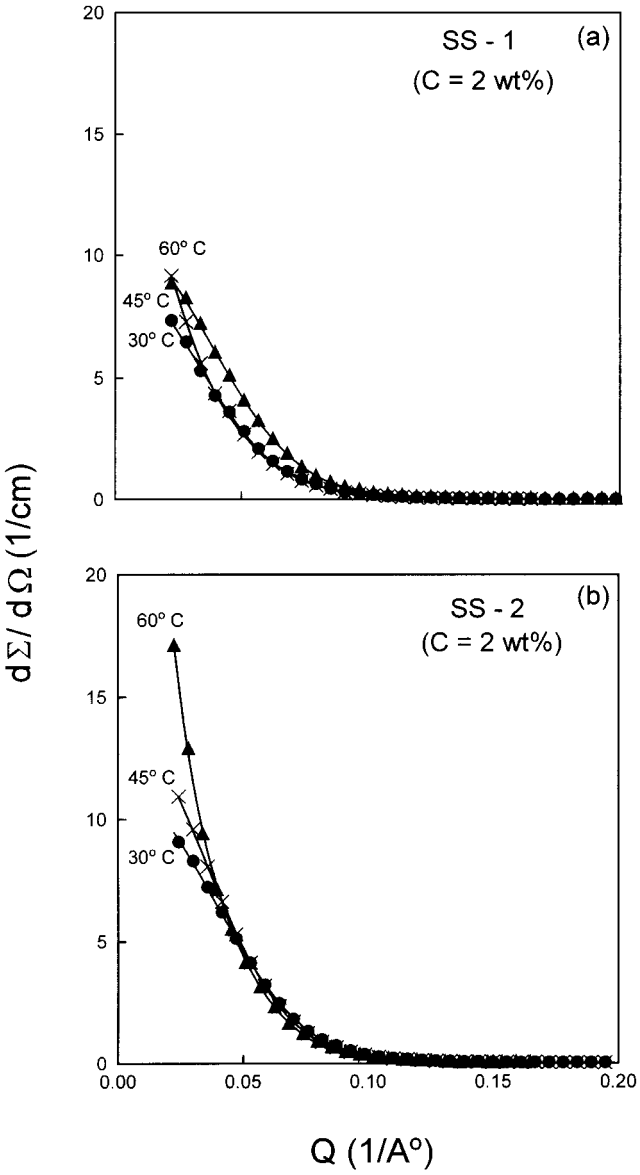

Figure 4. SANS distributions from micelles of 2 wt % silicone surfactant aqueous solution, (a) SS-1 and (b) SS-2, at different temperatures using the oblate ellipsoidal cross section formula of eq 11.

3.1.2b. Temperature Dependence. The scattering curves for a fixed concentration (2 wt %) of SS-1 and SS-2 aqueous solutions were also obtained at temperatures of 45 and 60 °C. The curves at 30, 45, and 60 °C are shown in parts a and b of Figure 4. It is seen that SANS intensities at large **Q** values are independent of temperature. However, at low **Q**, the SANS intensity increases as one approaches the cloud point. In principle, this could happen either because of a change in $\mathbf{F}(\mathbf{Q})$ (i.e., because of micellar growth) or because of a change in $\mathbf{S}(\mathbf{Q})$ (i.e., because of change in the intermicellar interaction potential). SANS data have been analyzed in the literature using both approaches, namely, one based on micellar growth or one based on divergence of $\mathbf{S}(\mathbf{Q})$. It seems SANS data cannot distinguish the two models though one can get certain param-

TABLE 4: Values of Semimajor Axis, b, Semiminor Axis, a, Axial Ratio, b/a, Aggregation Number, N_{agg}, and Number Density, n_m, of the Oblate Ellipsoidal Micelles of Silicone Surfactants at Different Temperatures

temp, °C	**b**, Å	**a**, Å	b/a	N_{agg}	$\mathbf{n}_m$, cm^{-3}
			SS-1		
30	50	23	2.2	92	3.007×10^{16}
45	56	23	2.4	114	2.427×10^{16}
60	64	23	2.6	147	1.881×10^{16}
			SS-2		
30	48	25	1.9	45	4.780×10^{16}
45	53	25	2.1	54	3.983×10^{16}
60	75	25	3.0	107	2.010×10^{16}

eters. We have interpreted the SANS data in terms of micellar growth for the following reasons: (i) the measured SANS distributions do not show a correlation peak, indicating that the intermicellar structure factor **S**(**Q**) is not important, and (ii) the viscocity data shows that there is a growth of the micelle as one approaches cloud temperature (see the next section).

Thus again, we analyzed the measured distributions of Figure 4 using eq 11 assuming ellipsoidal micelles. Because of the fact that large **Q** data are independent of temperature, the value of minor axis was fixed to **a** = 23 Å for SS-1 and **a** = 25 Å for SS-2 micelles. The micellar parameters at different temperatures are given in Table 4. It can be seen that the major axis **b** shows an increase of 28 and 56% with rise in temperature from 30 to 60 °C. Accordingly, the axial ratio **b**/**a** increases substantially. The data thus reveal that at a temperature of 60 °C [which is about and 4 and 14 °C close to the temperature at which the isotropic solutions turn turbid for SS-1 and SS-2 samples (see Figure 1)] the micelles elongate along the major axis without any change in their shape.

It is well established that, at elevated temperatures, dehydration effects not only cause conformational changes but also even disturb the geometry.[28] Extensive SANS measurements[29,32] on pluronic family of surfactants, L-81, P-85, F-87, F-88, and F-127, have been made. It has been reported that in most of the cases the micelles formed were of hard spherical in shape and that a rise in temperature (i) systematically increased various micellar parameters and (ii) will cause spherical micelles in some cases to even undergo a sphere to rod transition. Mesophases of higher order are also possible at higher concentrations. Similarly, several authors,[33−37] while analyzing SANS intensities from spherical micelles, allow for water in the core. Thus, both core as well as corona parts undergo dehydration at elevated temperatures.

Coming back to our SANS results at elevated temperatures on SS-1 and SS-2 surfactant solutions, we could not ascertain the information on the exact nature of the core and corona because of the poor contrast between the corona and the solvent medium. A look at columns 2, 5, and 6 (Table 4) reveals that the elongation along the major axis of the aggregates systematically increases the aggregation number, N_{agg}, and decreases the number density of the micelles at elevated temperatures. The increased N_{agg} values indicate that more surfactant molecules have been added into the space created because of the expulsion of water probably from the core as well as part of the corona portion of the micelles. The increased size of the aggregates as observed should decrease the number of aggregates in unit volume, i.e., number density. The broad spacing of the aggregates (low number density values) interspersed by water molecules (from bulk media) means absence of spatial correlation among the nearest neighbors, as evidenced by the absence of the correlation peak in curves shown in Figures 3 and 4. Finally, the observed elongation of the major axis could also be attributed to the loss of water (if any) from the core part, causing an expansion of hydrophobic siloxane chains or the merger of part of dehydrated PEO chains into the core part alongside the interface between the hydrophobic and hydrophilic regions.

The absolute magnitude of scattered intensities is found to be more for the aggregates formed by the SS-2 surfactant than SS-1 (see parts a and b of Figure 3). Not only this, the rise in intensities in the low **Q** region is sharp for SS-2 solutions. The SS-2 silicone surfactant has a molecular architecture (see Chart 1) having a close resemblance to a triblock copolymer (hydrophobic−hydrophilic−hydrophobic type). Thus, the dehydration effects at both the ends result in bigger sized particles as evidenced by higher **b** values of 75 Å (for SS-2) in comparison to a value of 64 Å (for SS-1) at 60 °C.

3.2. Viscosity Measurements. As noted earlier in our discussion, SANS measurements on silicone surfactant aqueous solutions showed that the micellar aggregates formed are oblate ellipsoidal in shape. We could not elicit direct information on the nature and extent of hydration from SANS analysis. The complex architecture of silicone surfactants makes it difficult to identify the separation of hydrophobic and hydrophilic parts of the aggregates in a clear and distinct manner. We assume that the core part of the aggregates is soft because of the possibility of hydration of Si−O groups and also the permeation of water into highly exposed core from the outer hydrophilic mantle consisting of ethylene oxide chains. The siloxane chains in the core part are expected to be in a coiled form because the semiminor axis values for both the surfactants never exceeded 23−25 Å under varying concentrations and temperatures. This value is far lower than the fully stretched lengths of 64 and 88 Å for the siloxane units of SS-1 and SS-2 surfactants. Hence, it is further assumed that water from the outer shell could be penetrated into the folds of the hydrophobic chains.

The absolute viscosities of aqueous solutions (for the concentrations of 1, 2, and 5 wt %) of SS-1 and SS-2 surfactants have been measured at the three temperatures at which SANS measurements were made. These experimentally obtained viscosities are compared with the theoretical viscosities calculated by using Einstein's formula $\eta = \eta_0 (1 + 2.5\phi)$ (which is applicable to hard spheres), where η_0 = the absolute viscosity of solutions at CMC and ϕ is the volume fraction of micelles (calculated from the ratio of the total micellar volume (obtained from SANS data) to volume of one molecule). The volume fractions, ϕ, η_{exp}, and η_{cal} (assuming spherical form) for SS-1 and SS-2 aqueous solutions under different conditions are shown in Table 5. The percentage standard deviation between experimental and calculated values as expected is too large and hence confirms that micellar aggregates are nonspherical in shape.

Viscosity measurements provide very useful information on the hydrodynamic volume of micellar aggregates. The hydrodynamic volume is proportional to intrinsic viscosities, $[\eta]$, of micellar solutions. The values of $[\eta]$ for SS-1 and SS-2 silicone surfactant micelles were obtained from the extrapolation of reduced viscosities to zero concentration following Huggins procedure. In addition of the measurement of the hydrodynamic volumes, the intrinsic viscosities are also very handy in calculating the hydration, *W*, i.e., a gram of water bound to a gram of surfactant. The following two equations have been widely used for calculating hydration values:[38,39]

$$W = \tilde{\nu}\rho_0\{(100[\eta]/2.5\tilde{\nu}) - 1\} \quad (15)$$

$$[\eta] = \upsilon(\tilde{\nu} + W\tilde{\nu}^0) \quad (16)$$

TABLE 5: Values of Micellar Volume Fraction, ϕ, Experimental Viscosities, η_{exp}, Calculated Viscosities, η_{cal}, and Percentage Standard Deviation, σ %, of Silicone Surfactant Aqueous Solutions at Different Concentrations and Temperatures

conc., wt %	temp, °C	ϕ	η_{exp}, cP	η_{cal}, cP	σ %
		SS-1			
1	30	0.006	0.786	0.784	0.38
2	30	0.011	0.818	0.794	3.05
2	45	0.023	0.671	0.633	6.07
2	60	0.033	0.522	0.470	9.98
5	30	0.023	0.929	0.816	12.16
		SS-2			
1	30	0.003	0.805	0.776	3.70
2	30	0.011	0.848	0.790	7.91
2	45	0.035	0.708	0.651	8.65
2	60	0.046	0.554	0.501	9.45
5	30	0.018	1.035	0.804	22.37

where $\tilde{\nu}$, ρ_0, $[\eta]$, and υ are the partial specific volume of surfactant, density of water, intrinsic viscosity, and shape factor of aggregates, respectively. The partial specific volume of the surfactant solute was calculated from the slope of the linear plots obtained by the equation $\rho = \rho_0 + (1 - \tilde{\nu}\rho_0)C$, where ρ is the density of solution at a given concentration, C. The calculation of hydration values using eq 15 assumes that the deviation in the shape of the aggregates from spheroids to nonspheroids is due to large hydration effects. Hence, results from this approach are approximations and are to be considered with caution. The estimated values of $[\eta]$, $\tilde{\nu}$, W, and υ at different temperatures are listed in Table 6. The rise in temperature increases systematically intrinsic viscosities. This result is in excellent agreement with the fact that aggregates in both the surfactants show elongation effects at elevated temperatures (see the SANS data in Table 4).

Most interestingly, the hydration values show a gradual increase with the temperature, and the increase is as much as two times in case of the SS-1 surfactant and 1.6 times for the SS-2 surfactant with a temperature rise from 30 to 60 °C. The hydration at any given temperature is more for aggregates of SS-2 than of the SS-1 surfactant. At first glance, the observed increasing trend in calculated hydration values for the aggregates at elevated temperatures is rather opposite to the usually expected reverse trend because of dehydration effects. However, a close look at eq 15 reveals that the hydration values must vary proportionately with the intrinsic viscosities which in turn are dependent highly on the size of the micellar aggregates.

With the substitution of the values of hydration as derived from eq 15 and the putting of the values of $[\eta]$, $\tilde{\nu}$, and $\tilde{\nu}^0$ into it, the shape factor, υ, can also be calculated using eq 16. The shape factor, υ, for ellipsoidal particles in fact is a function of the axial ratio **b**/**a** (υ is 2.5 for spheres and increases both for prolate and oblate ellipsoids[40]). A comparison of shape factors, as calculated from the combination of $[\eta]$ and hydration on one hand and from the axial ratios, obtained from the SANS data (Table 4), on the other hand, is presented in the last two columns of Table 6. The values of the shape factor calculated by both the approaches are more than 2.5, indicating unambiguously the nonspheroidal shape of the aggregates. The values of the shape factors evaluated by the above-mentioned two independent methods are reasonably close. The shape factors estimated from the axial ratios, as obtained from SANS intensities, take into consideration the hydrophobic core part only, whereas intrinsic viscosities of micelles have contributions both from the hydrophobic core as well as the hydrophilic outer shell. This difference in both of the approaches could be a reason for not obtaining identical values of shape factors for the same aggregates using two different methods.

The following explanation is given for the observed increased hydration of micellar aggregates at elevated temperatures. We propose that the oblate ellipsoidal aggregates of silicone surfactants probably have a soft core (i.e., hydrated) because of the Si−O group bound water and the fact that the distinction between the hydrophobic core and the hydrophilic outer mantle does not seem to be sharp. The water is also expected to be present in the interfacial region (between the hydrophobic core and hydrophilic shell), and of course, the outer shell of PEO is swollen with water. A rise in temperature then shall initiate the dehydration from within the core, the interfacial region, the inner part of the outer PEO mantle, and finally the PEO chains themselves. The very fact that the semimajor axis and aggregation number increase at elevated temperatures corroborates the above mechanism. As more and more water is expelled from the interior of the micelles, more and more surfactant molecules can be added and, hence, the rise in the aggregation number. The loss of water from the core and interfacial region further leads to elongation of micelles along the semimajor axis. The solutions of both the silicone surfactants at 60 °C are transparent and clear. Hence, it is logically presumed that the PEO outer shell and especially the outer part of the aggregates is still water swollen at 60 °C. The increased hydration with the rise in temperature up to 60 °C can thus be accounted for because of the expulsion of water from the core to the hydrophilic outer

TABLE 6: Intrinsic Viscosity, $[\eta]$, Partial Specific Volume, $\tilde{\nu}$, Hydration, W, Number of Water Molecules, and Simha Factor, υ, for Silicone Surfactant Micelles in Water at Different Temperatures

temp, °C	$[\eta]$, mL g^{-1}	$\tilde{\nu}$, mL g^{-1}	hydration, W, gm. of water/ gm. of surfactant	H_2O/ monomer	Simha factor, υ	
					$\upsilon = [\eta]/\tilde{\nu}$	from axial ratios of **b**/**a** (SANS)
			SS-1			
30	2.90	0.9236	0.24	58	3.14	4.47
40	3.15	0.9320	0.33	80	3.38	
45	3.25	0.9373	0.36	87	3.47	4.58
50	3.50	0.9432	0.45	109	3.71	
55	3.80	0.9393	0.57	138	4.05	
60	4.10	0.9478	0.68	165	4.33	4.76
			SS-2			
30	4.80	0.9178	0.99	308	5.22	4.36
40	5.70	0.9293	1.34	417	6.13	
45	5.80	0.9349	1.37	426	6.20	4.44
50	6.10	0.9516	1.47	457	6.42	
55	6.20	0.9607	1.51	470	6.45	
60	6.40	0.9752	1.60	498	6.57	4.88

shell. Such a preferential dehydration of hydrophobic PPO and hydrophilic PEO was also reported for the pluronic P-105 (EO_{37} PO_{58} EO_{37}) micelles in water by Guo et al.[41] The authors used deconvoluted FTIR spectra to gain microenvironmental information on PEO and PPO blocks. It was concluded that both the PPO core and PEO outer shell undergo dehydration at above 70 °C, and the PPO core is nearly anhydrous, whereas the PEO corona undergoes little dehydration, and moreover a substantial amount of water was reported to be present in the corona part at this elevated temperature. The dynamics of dehydration of complex micellar structures formed by amphiphilc block or branched copolymers need to be further probed thoroughly to give an explicit mechanism for the expulsion of water from the aggregates at elevated temperatures.

4. Conclusions

The silicone surfactants with a branched molecular architecture and based on polyether modified poly(dimethylsiloxane)s show unique and distinct phase, surface active, and aggregation behavior. Two silicone surfactants, SS-1 and SS-2, with varying ratios of 0.65 and 1.55 between hydrophobic and hydrophilic moieties were selected for detailed investigations using surface tension, SANS, and viscosity methods. The dilute aqueous phase behavior indicated that the solubility of both surfactants is mainly due to the hydrophilic ethylene oxide part. Upon heating, solutions become first turbid followed by appearance of cloudiness, which became denser at characteristic cloud points. No visible macrophase separation has been observed beyond the cloud point even up to 95 °C, indicating that otherwise water insoluble poly(dimethylsiloxane) is still dispersible in the presence of highly hydrophilic ethylene oxide moieties. The surface tension vs log concentration plots were found to be typically L shaped with a well defined single break point corresponding to CMC. The CMC values decreased systematically with an increase in hydrophobicity as well as with a rise in temperature. The surface areas at the air/water interface for silicone surfactants were in general larger than those of linear alkylpolyethers. The a_1^s almost remained invariant with the temperature for SS-1 molecules, whereas SS-2 molecules tended to occupy slightly more areas at elevated temperature. Hence, it is suggested that Si−O groups of hydrophobic parts of the molecule probably show a preferential orientation toward the water surface because of hydration. The free energy of micellization has always been negative, whereas enthalpies of micellization show a positive trend. Thus, it has been concluded that micellization is driven by an entropy factor.

The analysis of SANS intensities revealed that the aggregates are oblate ellipsoidal in shape. The axial ratio **b**/**a** remained almost invariant with the concentration at a given temperature without any change in geometry. Interestingly, SANS curves did not show any correlation peak in the low **Q** region, and absolute intensities were increased by 2−2.6 times at high concentration. Hence, it is thought that, the addition of more surfactant molecules results in a larger number of clusters in unit volume, i.e., an increase in number density of micelles. A rise in the temperature results in the dehydration of both the core and corona parts of the aggregates and thereby systematically elongates the semimajor axis, **b**, increases the aggregation number, N_{agg}, and decreases the number density of micelles. The calculated absolute viscosities considering a spherical shape for the aggregates differed largely with the experimental values, which confirm that aggregates have a nonspherical shape. The elongation of micelles along the semimajor axis, **b**, is also reflected in calculated intrinsic viscosities, which showed a gradual rise at elevated temperatures. The values of shape factors as obtained from SANS axial ratios on one hand and from viscosity measurements on the other have been found to be close.

Acknowledgment. We thank the Department of Atomic Energy, India, for the financial support of this work (Grant No. IUC/CRS-M-73/362-66). We also thank Dr. B. A. Dassanacharya for his useful suggestions and interest in this work.

References and Notes

(1) Chu, B.; Zhou, Z. Physical Chemistry of Polyalkylene Block Copolymer Surfactants. In *Nonionic Surfactants*. Nace, V. M., Ed.; *Surf. Sci. Ser.* **1996**, *60*, 67.

(2) Almgren, M.; Brown, W.; Hvidt, S. *Colloid Polym. Sci.* **1995**, *273*, 2.

(3) Alexandridis, P. *Curr. Opin. Colloid Interface Sci.* **1997**, *2*, 478.

(4) Booth, C.; Attwood, D. *Macromol. Rapid Commun.* **2000**, *21*, 501.

(5) Edens, M. W. Application of Polyoxyalkylene Block Copolymer Surfactants. In *Nonionic Surfactants.* Nace, V. M. Ed.; *Surf. Sci. Ser.* **1996**, *60,* 185.

(6) Chu, B. *Langmuir* **1995**, *11*, 414.

(7) Mortensen, K. *Curr. Opin. Colloid Interface Sci.* **1998**, *3*, 12.

(8) Schlachter, I.; Feldmann-Krane, G. Silicone Surfactants. In *Novel Surfactants Preparation, Application and Biodegradability*; Holmberg, K., Ed.; Marcel Dekker: New York, 1998; p 201.

(9) Kollmeier, H.-J.; Langenhagen, R. D. *Organo Polysiloxane Copolymers, Glodschmidt Informaiert* **1984**, *63*, 41.

(10) Gradzielski, M.; Hoffmann, H.; Robisch, P.; Ulbricht, W.; Gruning, B. *Tenside, Surf, Deterg.* **1990**, *27*, 366.

(11) Tegoprene−Silicone Surfactants. *Products, Data and Information, Technical Brochure*; Th. Goldschmidt AG: Essen, Germany, **1**990.

(12) Jain, D. V. S.; Singh, S. *Ind. J. Chem.* **1972**, *10*, 629.

(13) Riddick, J. A.; Bunger, W. B.; Sakano, T. K. *Organic Solvents*, 4th ed.; Wiley-Interscience: New York, 1986; Vol. II.

(14) Aswal, V. K.; Goyal, P. S. *Curr. Sci.* **2000**, *79*, 947.

(15) Rosen, M. J. *Surfactants and Interfacial Phenomena*, 2nd ed.; John Wiley and Sons: New York, 1989; p 67.

(16) Kanellopoulos, A. G.; Owen, M. J. *J. Colloid Interface Sci.* **1971**, *35*, 120.

(17) Wanka, G.; Hoffmann, H.; Ulbricht, W. *Colloid Polym. Sci.* **1990**, *268*, 101.

(18) Wanka, G.; Hoffmann, H.; Ulbricht, W. *Macromolecules* **1994**, *27*, 4145.

(19) Alexandridis, P.; Athanassiou, V.; Fukuda, F.; Hatton, T. A. *Langmuir* **1994**, *10*, 2604.

(20) Barry, B, W.; El Eini, D. I. D. *J. Colloid Interface Sci.* **1976**, *54*, 339.

(21) Meguro, K.; Takasawa, Y.; Kawahashi, N.; Tabata, Y.; Ueno, M. *J. Colloid Interface Sci.* **1981**, *83*, 50.

(22) Prasad, K. N.; Luong, T. T.; Florence, A. T.; Paris, J.; Vantion, C.; Seiller, M.; Puisieux., F. J. *J. Colloid Interface Sci.* **1979**, *69*, 225.

(23) Lo Nostro, P.; Gabrielli, G. *Langmuir* **1993**, *9*, 3132.

(24) (a) Chen, S. *H. Annu. Rev. Phys. Chem.* **1986**, *37*, 351. (b) Chen, S. H.; Lin, T. L. *Methods of Experimental Physics*; Academic Press: New York, 1987; Vol. 23 B, p 489.

(25) (a) Hayter, J. B.; Penfold, J. *Colloid Polym. Sci.* **1983**, *261*, 1022. (b) Hayter, J. B.; Penfold, *J. Mol. Phys.* **1981**, *42*, 109. (c) Hansen, J. P.; Hayter, J. B. *Mol. Phys.* **1982**, *46*, 109. (d) Hayter, J. B.; Penfold, J. *J. Chem. Soc. Faraday Trans. 1* **1981**, *77*, 1851.

(26) Goyal, P. S.; Rao, K. S.; Dasannacharya, B. A.; Kelkar, V. K. *Physica B* **1991**, *174*, 192.

(27) Goyal, P. S. *Phase Transitions* **1994**, *50*, 143.

(28) Goyal, P. S.; Menon, S. V. G.; Dasannacharya, B. A.; Thiyagarajan, P. *Phys. Rev. E* **1995**, *51*, 2308.

(29) Mortensen, K. *J. Phys. Condens. Matter* **1996**, *8*, A103.

(30) Jain, N. J.; Aswal, V. K.; Goyal, P. S.; Bahadur, P. J. *Phys. Chem. B* **1998**, *102*, 8452.

(31) Israelachivili, I. N.; Mitchell, D. J.; Ninham, B. W. *J. Chem. Soc., Faraday Trans. 2* **1976**, *72*, 1525.

(32) Mortensen, K.; Talmon, Y. *Macromolecules* **1995**, *28*, 8829.
(33) Derici, L.; Ledger, S.; Mai, S.-M.; Booth, C.; Hamley, I. W.; Pedersen, J. S. *Phys. Chem. Chem. Phys.* **1999**, *1*, 2773.
(34) Goldmints, I.; von Gottberg, F. K.; Smith, K. A.; Hatton, T. A. *Langmuir* **1997**, *13*, 3659.
(35) Goldmints, I.; Yu, G.-E.; Booth, C.; Smith, K. A.; Hatton, T. A. *Langmuir* **1999**, *15*, 1651.
(36) Liu, Y. C.; Chen, S. H.; Huang, J. S. *Physica B* **1998**, *243*, 1019.
(37) Pedersen, J. S.; Gerstenberg, M. C. *Macromolecules* **1996**, *29*, 1363.
(38) Tokiwa, F.; Okhi, K. *J. Phys. Chem.* **1967**, *71*, 1343.
(39) Oncley, J. L. *Ann. N.Y. Acad. Sci.* **1940**, *41*, 121.
(40) Simha, R. *J. Phys. Chem.* **1940**, *44*, 25.
(41) Guo, C.; Liu, H. Z.; Chen, J. Y. *Colloid Polym. Sci.* **1999**, *277*, 376.